REGULAR PAPER



Ai-enabled efficient modulation classification in underwater OWC systems

Qingwen He¹ · Zhihong Zeng¹ · Min Liu¹ · Binbin Zhu² · Bangjiang Lin³ · Chen Chen¹

Received: 4 June 2024 / Accepted: 3 October 2024 © The Optical Society of Japan 2024

Abstract

In this paper, we propose and experimentally demonstrate an artificial intelligence (AI)-enabled efficient modulation classification technique for underwater optical wireless communication (UOWC) systems. Specifically, time-domain waveform histograms are adopted as classification features, where three modulation formats including direct current biased optical orthogonal frequency division multiplexing (DCO-OFDM), asymmetrically clipped optical OFDM (ACO-OFDM) and pulse amplitude modulation (PAM) are considered. Moreover, AI algorithms such as decision trees (DT), k-nearest neighbors (k-NN), support vector machines (SVM) and convolutional neural networks (CNN) are utilized to realize efficient modulation classification based on the obtained waveform histogram features. Experimental results demonstrate that all the four algorithms can achieve accuracy surpassing 95% when the received signal-to-noise ratio (SNR) exceeds 6.3 dB. Furthermore, increasing the number of symbols in histograms enhances classification accuracy, whereas altering the number of histogram bins has minimal impact on classification accuracy.

Keywords Underwater optical wireless communication (UOWC) · Modulation classification · Orthogonal frequency division multiplexing (OFDM) · Pulse amplitude modulation (PAM)

1 Introduction

Underwater optical wireless communication (UOWC) achieved a significant breakthrough following the development of the AquaOptical II underwater optical communication system by Marek and Daniela, which utilized light-emitting diode (LED) arrays [1]. UOWC offers notable advantages including high data rates, low delay, high communication security, substantial transmission capacity, and cost-effective implementation. Consequently, it has emerged as a focal point in research within the realm of underwater information transmission [2]. Despite its many advantages,

still faces many challenges including limited modulation bandwidth of LED sources, water turbidity, and turbulence [3]. So far, several techniques have been reported to enhance the performance of UOWC systems such as spatial division transmission and pairwise coding [4], and multi-dimensional transmission exploiting frequency, wavelength and polarization for robust and high-speed underwater data transmission [5, 6].

the practical application of UOWC in real-world scenarios

Particularly, the orthogonal frequency division multiplexing (OFDM) technique has attracted considerable attention in UOWC recently, primarily due to resistance to inter-symbol interference (ISI) and high spectral efficiency [7]. In UOWC systems, where the transmitters utilize LEDs or laser diodes (LDs) as non-coherent light sources, intensity modulation with direct detection (IM/DD) is typically employed for signal transmission. As a result, OFDM signals in UOWC systems are constrained to convey as unipolar signals, meaning they are real and non-negative [8]. Presently, several popular optical OFDM formats have been proposed for IM/DD systems, which mainly include direct current biased optical OFDM (DCO-OFDM) and asymmetrically clipped optical OFDM (ACO-OFDM) [9]. To ensure that

☑ Zhihong Zeng zhihong.zeng@cqu.edu.cn

Published online: 14 October 2024

- School of Microelectronics and Communication Engineering, Chongqing University, 400044 Chongqing, China
- Shenzhen Hua Chuang Chip Lighting Company, Ltd, 518027 Shenzhen, China
- Quanzhou Institute of Equipment Manufacturing, Haixi Institutes, Chinese Academy of Sciences, Quanzhou, Fujian, China

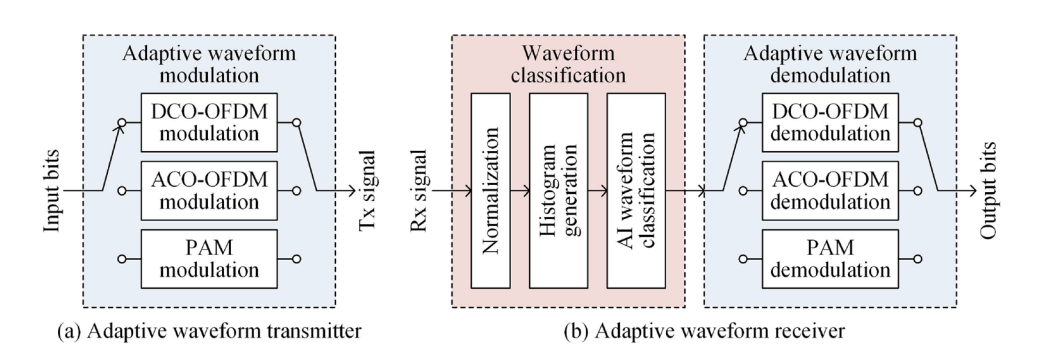


OFDM signals are real, the Hermitian symmetry condition is applied to the subcarrier data symbols. To prevent negative signals, DCO-OFDM introduces a direct current (DC) bias and zero clipping. In the case of ACO-OFDM, only odd frequency subcarriers are utilized for carrying symbols, while even frequency subcarriers are set to zero. Consequently, zero clipping noise only appears on the even subcarriers. In brief, DCO-OFDM is more spectrally efficient while ACO-OFDM is more power efficient [10–12]. Besides optical OFDM schemes, pulse amplitude modulation (PAM) is also commonly applied in UOWC due to its low computational complexity, low peak-to-average power ratio (PAPR), and simple structure [13, 14].

In practical UOWC systems, the underwater channel can be very dynamic and diverse communication requirements might be required in various scenarios. Hence, besides conventional adaptive constellation modulation [15], adaptive waveform modulation can also be applied to enhance the performance of practical UOWC systems by fully utilizing the advantages of different OFDM and PAM modulation formats. When UOWC transmitters switch among different OFDM and PAM modulation formats, an efficient modulation classification technique is of practical significance to identify and adjust the corresponding demodulation scheme [16]. Although constellation classification has been studied for adaptive UOWC systems [17], it is not applicable to realize modulation classification among various OFDM and PAM formats. To the best of our knowledge, efficient modulation classification among various OFDM and PAM formats has not yet been reported for adaptive UOWC systems in the literature so far, which remains to be an open problem in the field of UOWC.

Recently, artificial intelligence (AI) including traditional machine learning and deep learning has been extensively applied for performance improvement of UOWC systems, e.g., deep learning-aided robust joint channel classification, channel estimation and signal detection [18], reinforcement-learning-based beam adaptation [19], sparse weight-initiated deep neural network (DNN) equalization [20], neural equalization for 512-color shift keying signal demodulation in optical camera communication [21], deep learning-based link adaptation [22], intelligent index

Fig. 1 Schematic diagram of adaptive waveform transmission in UOWC systems: **a** adaptive waveform transmitter and **b** adaptive waveform receiver



recognition using AI for OFDM with index modulation in underwater OWC systems [23], ResNet-based real-time beam tracking in water-air OWC systems [24], and long short term memory neural network (LSTM-NN) enabled optical camera communication for field-of-view (FOV) water-to-air transmission [25]. In this paper, we propose an efficient modulation classification technique for UOWC systems by exploring the time-domain waveform histograms as classification features and utilizing AI algorithms such as decision trees (DT), *k*-nearest neighbors (*k*-NN), support vector machines (SVM) and convolutional neural networks (CNN) to perform modulation classification. Experimental results demonstrate that accurate modulation classification is achievable under a sufficiently high signal-to-noise ratio (SNR).

2 Principle

Figure 1 illustrates the schematic diagrams of adaptive waveform transmission in UOWC systems. The selection of waveform modulation format for the transmitted signal depends on channel conditions and the dynamic range of the transmitter (Tx). Upon reception, after normalizing the instantaneous amplitude values of the received signal, histogram data is acquired. This data is then fed into a pre-trained classification model, which outputs the classification results. Based on these results, the signal demodulator selects the appropriate demodulation scheme to recover the original signal.

In this study, four classical AI algorithms including DT, *k*-NN, SVM and CNN are employed. Histograms, represented as an *H*-dimensional real vector, are utilized as features for efficient modulation classification using AI algorithms [26–28]. For each AI algorithm, the histogram dataset from three modulation formats, i.e., DCO-OFDM, ACO-OFDM and PAM, is divided into training and testing datasets, respectively.

DT: A complete decision tree is composed of a root node containing all histogram data and modulation formats. It includes several process nodes indicating feature



determination, with corresponding leaf nodes representing decision results.

k-NN: *k*-NN works by calculating the similarity between testing and training histogram data. It identifies the *k* nearest neighbors based on this similarity measure. Subsequently, the labels of these neighbors are voted to determine the modulation formats.

SVM: SVM maps the input histogram data into a high dimensional feature space. Within this space, a linear decision surface is constructed to separate different classes. While the SVMs are inherently binary classifiers, they can facilitate multi-category classification by combining multiple binary classifiers.

CNN: CNN is a type of deep feed-forward neural network commonly used for image classification tasks. Utilizing 2D convolutional layers, CNNs can effectively extract various features from histogram data. As the weights of the CNN models are updated and further optimized, the classification accuracy of modulation formats tends to improve. This enhancement in accuracy contributes to better generalization performance of the CNN model.

3 Experimental setup and results

3.1 Experimental setup

Figure 2 illustrates the experimental setup of a point-topoint UOWC system employing a vertical-cavity surfaceemitting laser (VCSEL) as the Tx end. The transmitted

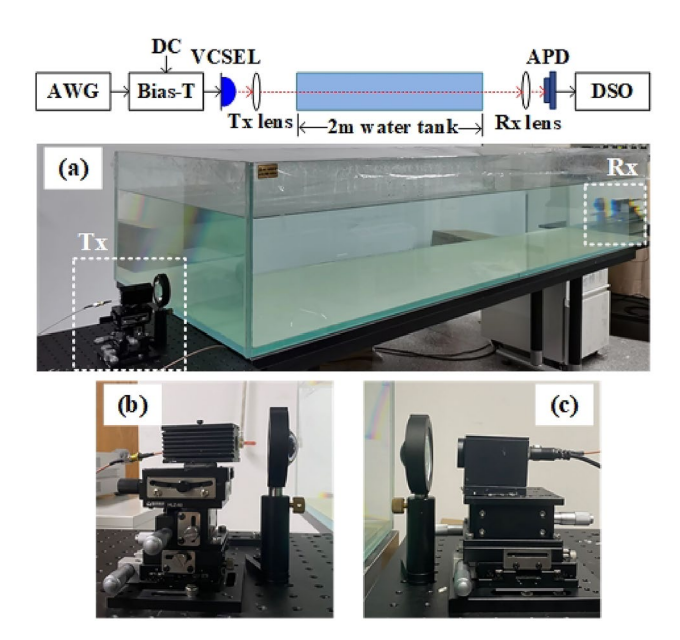


Fig. 2 Experimental setup of a point-to-point UOWC system using a red VCSEL. Insets: photos of **a** the overall system, **b** the transmitter, and **c** the receiver

signal, generated offline using MATLAB, is loaded onto an arbitrary waveform generator (AWG, Tektronix AWG7101), ensuring that the bandwidth of both signals is about 1 GHz. Subsequently, a 230-mA DC bias current is applied via a bias-tee (bias-T, Mini-circuit ZFBT-6GW+) to drive a red VCSEL (DERAY DV0688M). The emitted light propagates sequentially through the Tx lens, the underwater channel and the receiver (Rx) lens. At the Rx end, an avalanche photodiode (APD, Menlo Systems APD210) with a bandwidth of 1 GHz detects the optical signal. The detected signal is then captured by a digital storage oscilloscope (DSO, Tektronix MSO73304DX). Offline demodulation is subsequently performed using MATLAB.

The key parameters of the experiments are detailed in Table 1. The underwater transmission distance is set to 2 ms. For the OFDM signal, the IFFT/FFT length is set to 64. In order to achieve the same transmission rate for the three modulated formats, DCO-OFDM symbols employ 2QAM, ACO-OFDM symbols use 4QAM, and the single carrier signal employs 2-PAM modulation. Subsequently, the received signal values are normalized to fall within the range of [0, 1]. Furthermore, 400 symbols are generated for each modulation format, and the resulting 1200 *H*-dimensional vector dataset is partitioned into training and testing datasets with a ratio of 4:1. The primary performance metric in this study is classification accuracy, calculated by averaging the accuracies of 50 tests for each classification algorithm.

3.2 Measured waveform histograms

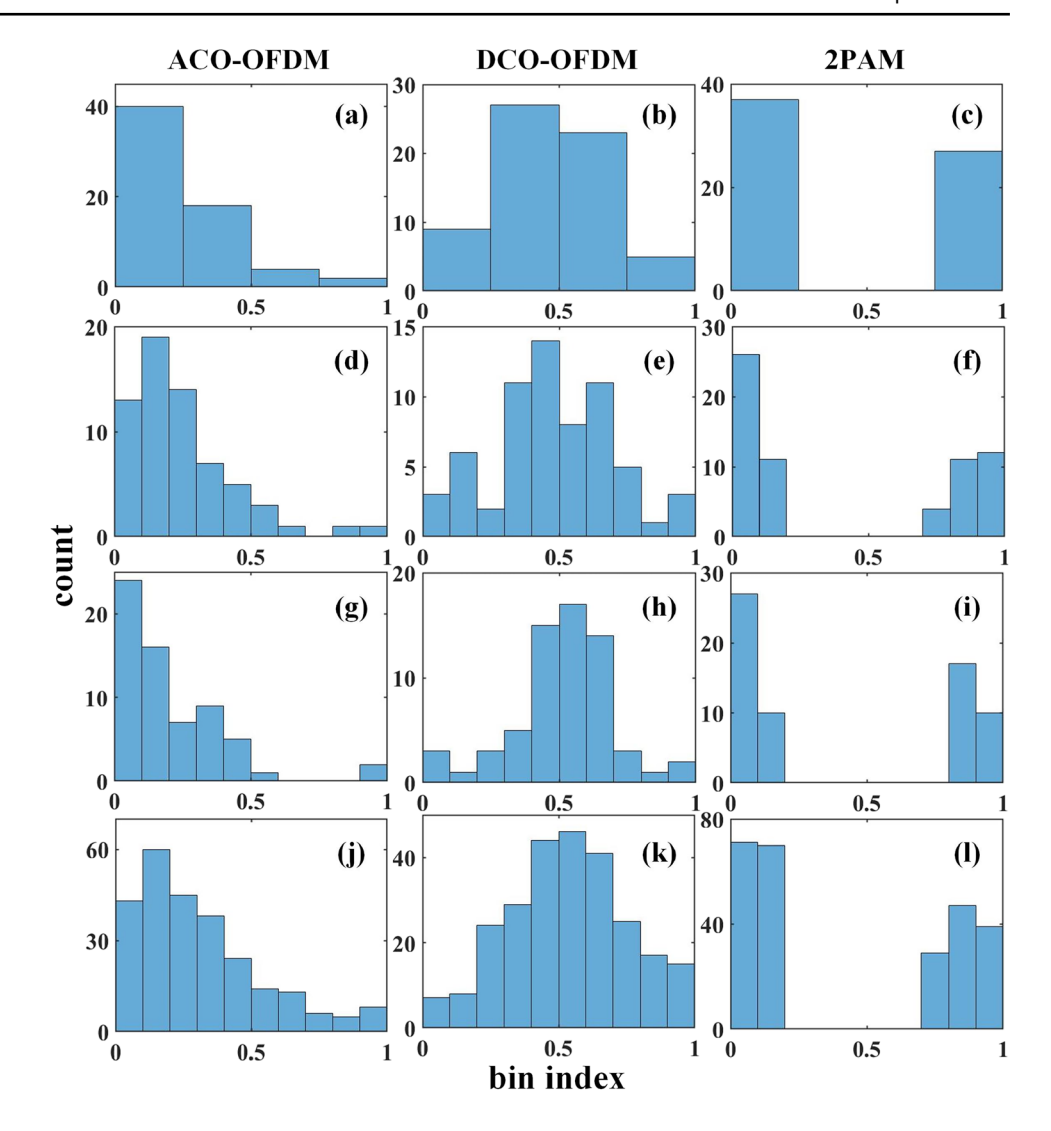
Let SNR, H and $N_{\rm sym}$ represent the estimated SNR at the Rx end, the number of histogram bins and the number of symbols included in the histogram, respectively. Figure 3 shows the waveform histograms of three modulation formats with different SNR, H and $N_{\rm sym}$ values. As we can see, distinct histogram shapes emerge among ACO-OFDM, DCO-OFDM, and PAM, facilitating waveform classification. The histogram of ACO-OFDM tend to concentrate around 0, DCO-OFDM signals around 0.5, while PAM signals cluster around 0 and 1. Moreover, the peak and shape of the histogram begin to shift and the histogram shapes among different modulation formats become

Table 1 Experimental parameters

Parameter	Value
IFFT/FFT size	64
Number of symbols	400
Constellation for DCO-OFDM	2QAM
Constellation for ACO-OFDM	4QAM
DC bias	230 mA
Transmission distance	2 m
Signal bandwidth	1 GHz



Fig. 3 Waveform histograms: a ACO-OFDM, SNR = 3.7 dB, H= 4, N_{sym} = 1, **b** DCO-OFDM, $SNR = 3.7 \text{ dB}, H = 4, N_{sym} =$ 1, **c** PAM, SNR = 3.7 dB, H =4, $N_{sym} = 1$, **d** ACO-OFDM, $SNR = 3.7 \text{ dB}, H = 10, N_{sym} =$ 1, e DCO-OFDM, SNR = 3.7dB, H = 10, $N_{sym} = 1$, **f** PAM, SNR = 3.7 dB, H = 10, N_{sym} $= 1, \mathbf{g}$ ACO-OFDM, SNR = $10.2 \text{ dB}, H = 10, N_{sym} = 1, \mathbf{h}$ DCO-OFDM, SNR = 10.2 dB, H = 10, $N_{sym} = 1$, **i** PAM, SNR= 10.2 dB, H = 10, $N_{sym} = 1$, **j** ACO-OFDM, SNR = 3.7 dB, H= 10, N_{sym} = 4, **k** DCO-OFDM, $SNR = 3.7 \text{ dB}, H = 10, N_{sym} =$ 4, and I PAM, SNR = 3.7 dB, H $= 10, N_{sym} = 4$



less distinct at lower SNR levels. It can be concluded from Fig. 3 that it is effective to employ the time-domain waveform histograms as distinctive features to perform classification for different modulation formats.

3.3 Impact of received SNR

Figure 4 presents the classification accuracy achieved by four AI classification algorithms across various received SNR values. It is evident that the accuracy of all four algorithms increases steadily with rising SNR. Notably, SVM consistently demonstrates higher accuracy compared to other algorithms when SNR is below 3.7 dB. Furthermore, for SNR = 10.2 dB, SVM achieves an impressive accuracy of 99.62%.

3.4 Impact of symbol number

To enhance classification accuracy at low SNR levels, we construct new histograms with an increased number of symbols for OFDM signals. Correspondingly, the number of symbols

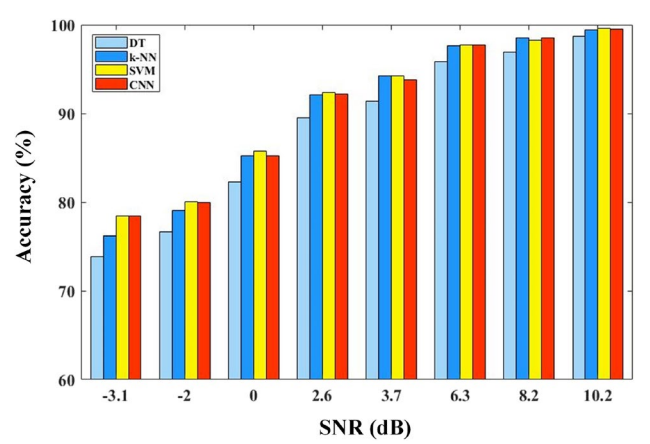


Fig. 4 Classification accuracy in percentage vs. received SNR (SNR) in dB for four AI classification algorithms with H=10 and $N_{\rm sym}=1$

for transmitted PAM signals is increased by the same multiple. Figure 3j–l compare histograms of different modulation formats after adjusting N_{sym} , with SNR set at 3.7 dB and H=10.



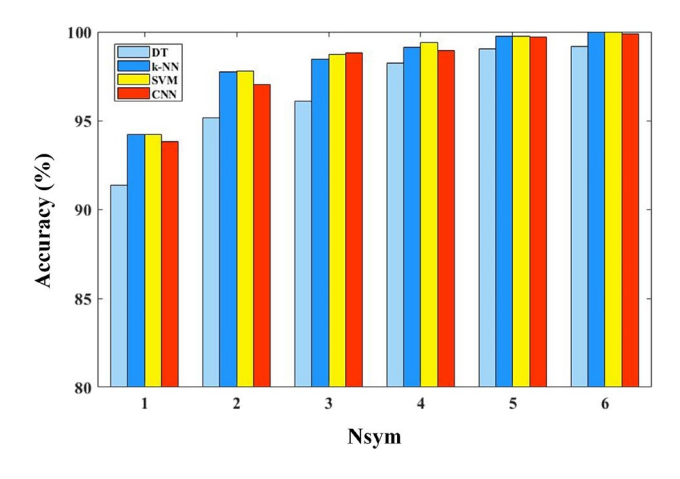


Fig. 5 Classification accuracy in percentage vs. number of symbols (N_{sym}) for four AI classification algorithms with SNR = 3.7 dB and H = 10

As illustrated in Fig. 5, augmenting $N_{\rm sym}$ results in improved accuracy across all four classification algorithms. Notably, both k-NN and SVM achieve 100% accuracy for $N_{\rm sym}=6$ at low SNR of 3.7 dB. This represents a substantial improvement compared to the 94.21% accuracy of k-NN and 94.23% accuracy of SVM for $N_{\rm sym}=1$, marking a 5.8% increase in accuracy. The observed enhancement can be attributed to the instability of individual signal values at low SNR levels, where histogram shapes exhibit minimal variation, thereby affecting classification performance. However, increasing $N_{\rm sym}$ results in more distinct histogram shapes.

3.5 Impact of bin number

We further investigate the impact of the number of histogram bins (H) on classification accuracy. In Fig. 3a–f, we compare histogram shapes between two scenarios: H=4 and H=10, with SNR set at 3.7 dB and $N_{\rm sym}=1$. Observing the histograms, we note that with H=4, shapes become more concentrated in one bin, leading to increased values in each bin and greater fluctuation among neighboring bins compared to H=10. Figure 6 illustrates the classification accuracy achieved by four classification algorithms for various numbers of histogram bins. Interestingly, altering H from 3 to 12 does not significantly enhance performance across all classification algorithms, which might due to the fact that a bin number of 3 is sufficiently enough for the time-domain waveform histograms to extract the distinctive features for different OFDM and PAM modulation formats.

3.6 Comparison and discussions

Generally speaking, modulation classification techniques fall into two main categories: one is likelihood-based

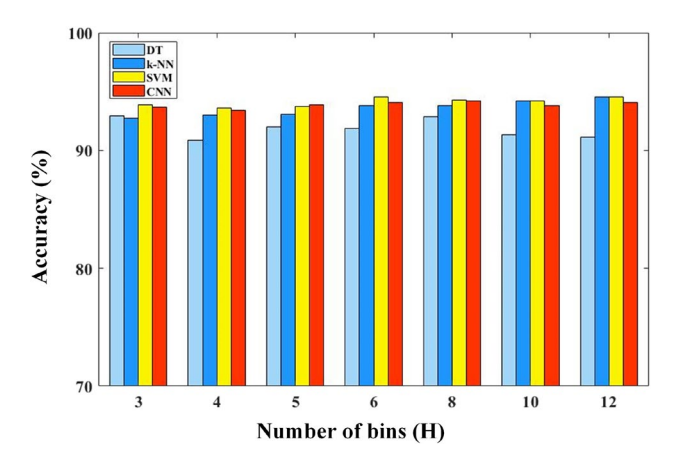


Fig. 6 Classification accuracy in percentage vs. number of bins (H) for four AI classification algorithms with SNR = 3.7 dB and $N_{sym} = 1$

classification and the other is feature-based classification. Particularly, likelihood-based classification usually requires relatively high computational complexity to calculate the likelihood ratios which might limit its practical applications, while conventional feature-based classification normally needs a lot of data for training so as to obtain satisfactory classification performance [29, 30]. In contrast, the proposed AI-enabled efficient modulation classification technique employing time-domain waveform histograms is shown to be a low-complexity way to achieve robust classification with reduced training requirement. Hence, the proposed efficient modulation classification technique has the potential for practical implementation in real-world UOWC systems.

4 Conclusion

This paper presents experimental demonstrations of classification among DCO-OFDM, ACO-OFDM, and PAM for point-to-point UOWC systems. The histogram shapes vary for different modulated signals, providing valuable information for a feature-based classifier. Four classical classification algorithms were employed, achieving accuracy exceeding 95% when the received SNR surpasses 6.3 dB. Notably, SVM outperforms DT, k-NN, and CNN, particularly at relatively low SNR levels. Additionally, we found that increasing the number of symbols in histogram data improves classification accuracy, while altering the number of histogram bins has minimal impact on classifications. Hence, selecting the appropriate classification algorithms for received signals enables the receiver to accurately identify modulation formats and then adjust demodulation formats, thereby promoting efficient and high-quality communication.

In our future work, we will consider the efficient classification of more types of modulation formats in



UOWC systems applying adaptive waveform transmission. Moreover, joint classification of waveform formats and constellation formats will also be further investigated for intelligent UOWC systems.

Acknowledgements This work was supported by the National Natural Science Foundation of China (Grant No. 62271091).

Code and Data Availability Data sharing is not applicable to this article, as no new data were created or analyzed.

Declarations

Conflict of interest The authors declare that there are no Conflict of interest related to this article.

References

- Doniec, M., Rus, D.: Bi-directional optical communication with AquaOptical II. In: IEEE International Conference on Communication Systems, 390–394 (2010)
- Wang, K., Zhou, Z., Rotenberg, S., et al.: Demonstration of remote underwater monitoring using underwater wireless communication and satellite system. Eur. Conf. Opt. Commun. (ECOC) 2023, 1472–1475 (2023)
- Xu, J., Zhang, Y., Cai, C.: Underwater wireless optical communications: From the lab tank to the real sea. In: Optical Fiber Communications Conference and Exhibition (OFC), 1–3 (2024)
- Wang, J., Chen, C., Deng, B., et al.: Enhancing underwater VLC with spatial division transmission and pairwise coding. Opt. Express 31(10), 16812–16832 (2023)
- Deng, B., Wang, J., Wang, Z., et al.: Polarization multiplexing based UOWC systems under bubble turbulence. J. Lightwave Technol. 41(17), 5588–5598 (2023)
- Deng, B., Chen, C., Huang, H., et al.: Three-dimensional transmission based UOWC in complex underwater environments. J. Lightwave Technol. (2024)
- Lian, J., Gao, Y., Wu, P., et al.: Orthogonal frequency division multiplexing techniques comparison for underwater optical wireless communication systems. Sensors 19(1), 160 (2019)
- Elgala, H., Mesleh, R., Haas, H.: Indoor optical wireless communication: potential and state-of-the-art. IEEE Commun. Mag. 49(9), 56–62 (2011)
- Armstrong, J., Schmidt, B.J.: Comparison of asymmetrically clipped optical OFDM and DC-biased optical OFDM in AWGN. IEEE Commun. Lett. 12(5), 343–345 (2008)
- Sohail, M., Saengudomlert, P., Sterckx, K.L.: Performance analysis of dynamic range limited DCO-OFDM, ACO-OFDM and Flip-OFDM transmissions for visible light communication. IEICE Trans. Commun. 97(10), 2192–2202 (2014)
- Hassan, R., Tuli, F. T. Z.: Analysis of ACO-OFDM, DCO-OFDM and Flip-OFDM for IM/DD optical-wireless and optical-fiber system. In: IEEE International Conference on Telecommunications and Photonics (ICTP), 1–5 (2015)
- Ullah, H., Sohail, M., Bokhari, M.: Dynamic range of LED in optical OFDM for PAPR performance analysis. Opt. Quant. Electron. 54(11), 742 (2022)
- Lian, J., Noshad, M., Brandt-Pearce, M.: M-PAM joint optimal waveform design for multiuser VLC systems over ISI channels. J. Lightwave Technol. 36(16), 3472–3480 (2018)
- Chi, N., Shi, M., Wang, C., et al.: High speed visible light communication based on pulse amplitude modulation. In: International conference on optical communications and networks (ICOCN), 1–3 (2017)

- Fei, C., Hong, X., Du, J., et al.: High-speed underwater wireless optical communications: from a perspective of advanced modulation formats. Chin. Opt. Lett. 17(10), 100012 (2019)
- Saengudomlert, P., Buddhacharya, S.: Modulation classification between DCO-OFDM and Flip-OFDM for visible light communications. In: International Technical Conference on Circuits/Systems, Computers and Communications (ITC-CSCC), 1–4 (2022)
- Xu, C., Jin, R., Gao, W., et al.: Efficient modulation classification based on complementary folding algorithm in UVLC system. IEEE Photonics J. 14(4), 1–6 (2022)
- Lu, H., Jiang, M., Cheng, J.: Deep learning aided robust joint channel classification, channel estimation, and signal detection for underwater optical communication. IEEE Trans. Commun. 69(4), 2290–2303 (2020)
- Romdhane, I., Kaddoum, G.: A reinforcement-learning-based beam adaptation for underwater optical wireless communications. IEEE Internet Things J. 9(20), 20270–20281 (2022)
- Du, Z., Ge, W., Cai, C., et al.: 90-m/660-Mbps underwater wireless optical communication enabled by interleaved single-carrier FDM scheme combined with sparse weight-initiated DNN equalizer. J. Lightwave Technol. 41(16), 5310–5320 (2023)
- Onodera, Y., Hisano, D., Maruta, K., et al.: First demonstration of 512-color shift keying signal demodulation using neural equalization for optical camera communication. In: Optical Fiber Communication Conference, Th3H–7 (2023)
- Zhao, X., Qi, Z., Pompili, D.: Link adaptation in underwater wireless optical communications based on deep learning. Comput. Netw. 242, 110233 (2024)
- Zhang, X., Zeng, Z., Du, P., et al.: Intelligent index recognition for OFDM with index modulation in underwater OWC systems. IEEE Photonics Technol. Lett. 36(20), 1249–1252 (2024)
- 24. Xu, A., Di, Y., Yue, X., *et al.*: Seeing through wave–Real-time beam tracking via a ResNet-based model in water-air OWC systems. In: Optical Fiber Communications Conference and Exhibition (OFC), 1–3 (2024)
- Chang, Y.-H., Tsai, S.-Y., Tsai, M.-C., et al.: Water-to-air PAM4 optical camera communication using long short term memory neural network (LSTM-NN). In: Optical Fiber Communications Conference and Exhibition (OFC), 1–3 (2024)
- Kotsiantis, S.B., Zaharakis, I.D., Pintelas, P.E.: Machine learning: a review of classification and combining techniques. Artif. Intell. Rev. 26, 159–190 (2006)
- 27. LeCun, Y., Bengio, Y., Hinton, G.: Deep learning. Nature **521**(7553), 436–444 (2015)
- Krizhevsky, A., Sutskever, I., Hinton, G.E.: ImageNet classification with deep convolutional neural networks. Commun. ACM 60(6), 84–90 (2017)
- Huang, Z., Zhang, Q., Xin, X., et al.: Modulation format identification based on signal constellation diagrams and support vector machine. Photonics 9(12), 927 (2022)
- Zhao, Z., Khan, F.N., Li, Y., et al.: Application and comparison of active and transfer learning approaches for modulation format classification in visible light communication systems. Opt. Express 30(10), 16351–16361 (2022)

Publisher's Note Springer Nature remains neutral with regard to jurisdictional claims in published maps and institutional affiliations.

Springer Nature or its licensor (e.g. a society or other partner) holds exclusive rights to this article under a publishing agreement with the author(s) or other rightsholder(s); author self-archiving of the accepted manuscript version of this article is solely governed by the terms of such publishing agreement and applicable law.

